

Adhesion Improvement of Thermoplastics-Based Composites by Atmospheric Plasma and UV Treatments

Scarselli, Gennaro; Quan, Dong; Murphy, Neal; Deegan, Brian; Dowling, Denis; Ivankovic, Alojz

DOI

[10.1007/s10443-020-09854-y](https://doi.org/10.1007/s10443-020-09854-y)

Publication date

2021

Document Version

Final published version

Published in

Applied Composite Materials

Citation (APA)

Scarselli, G., Quan, D., Murphy, N., Deegan, B., Dowling, D., & Ivankovic, A. (2021). Adhesion Improvement of Thermoplastics-Based Composites by Atmospheric Plasma and UV Treatments. *Applied Composite Materials*, 28(1), 71-89. <https://doi.org/10.1007/s10443-020-09854-y>

Important note

To cite this publication, please use the final published version (if applicable). Please check the document version above.

Copyright

Other than for strictly personal use, it is not permitted to download, forward or distribute the text or part of it, without the consent of the author(s) and/or copyright holder(s), unless the work is under an open content license such as Creative Commons.

Takedown policy

Please contact us and provide details if you believe this document breaches copyrights. We will remove access to the work immediately and investigate your claim.



Adhesion Improvement of Thermoplastics-Based Composites by Atmospheric Plasma and UV Treatments

Gennaro Scarselli^{1,3} · Dong Quan² · Neal Murphy³ · Brian Deegan⁴ · Denis Dowling³ · Alojz Ivankovic³

Received: 11 August 2020 / Accepted: 17 November 2020
© The Author(s) 2020

Abstract

The present work is concerned with adhesive bonding of thermoplastic composites used in general aerospace applications, including polyphenylene sulfide (PPS), polyetherimide (PEI) and polyetheretherketone (PEEK) carbon fibre composites. Three different surface treatments have been applied to the PEEK, PPS and PEI-based composites in order to enhance the adhesion: atmospheric plasma, ultraviolet radiation (UV) and isopropanol wiping as a control. Water contact angles and free surface energies were measured following the standard experimental procedure based on the employment of three different liquid droplets. Infrared spectroscopy and X-ray photoelectron spectroscopy (XPS) were subsequently performed to characterize the surface chemistry of the samples after treatment. The single lap joints were manufactured and bonded by an Aerospace grade epoxy-based film adhesive originally developed for use on metals but with the ability to bond treated thermoplastics to good strength (supplied by Henkel Ireland). Quasi-static (QS) tests were conducted. The lap shear strength was evaluated, and the failure mechanisms of the different joints were examined for the range of surface treatments considered. It was found that the performances of the PEEK and PPS joints were considerably improved by the plasma and UV treatments resulting in cohesive and delamination failures, while PEI was unaffected by the plasma and UV treatments and performed very well throughout.

Keywords Thermoplastics · Adhesion · UV treatment · Atmospheric plasma treatment

✉ Dong Quan
D.Quan-1@tudelft.nl

¹ Department of Engineering for Innovation, University of Salento, Via per Monteroni, Lecce, Italy

² Structural Integrity & Composites Group, Faculty of Aerospace Engineering, Delft University of Technology, Delft, Netherlands

³ School of Mechanical and Materials Engineering, University College Dublin, Belfield, Dublin, Ireland

⁴ Adhesives Research, Henkel Ireland Operations & Research Ltd., Tallaght, Dublin, Ireland

1 Introduction

The increasing use of polymer composites in a wide variety of industrial applications has resulted in a corresponding interest in the most effective ways by which these materials may be joined together. It is well recognized that the use of structural adhesives offers distinct potential advantages over mechanical fastening techniques such as bolting or riveting which result in localized damage of the fibre-reinforced laminates. In recent years, thermoplastic composites (TPC) have received considerable attention due to their superior fracture toughness, processing advantages and recyclability compared to their classical thermosetting counterparts. One of the drawbacks of this category of materials is the relative difficulty experienced in forming a high quality adhesive bond between the thermoplastic substrates [1]. As a result, ongoing attempts have been made to investigate appropriate surface treatments to improve their adhesion characteristics. Thermoplastic surfaces are innately hydrophobic, meaning that they will repel any liquid they meet. For adhesive bonding, the quality of a bond depends on the adhesive's ability to spread over the required area. So, to create a strong, uniform bond, surface treatments must be performed to make the surface more hydrophilic in nature. Most surface treatments improve adhesion properties by increasing the surface free energy of the material [2, 3]. Many studies have linked solid bond creation with surface energy that is essentially the excess energy associated with a surface [4, 5]. The surface of the material will always be less energetically favourable than the bulk, otherwise, there would be a constant driving force for new surfaces to be created. Increased surface energy will generally coincide with increased wettability, allowing for a better spread of the adhesive [6]. Plasma is a gaseous mixture of ions, radicals, electrons and neutrals, distinguished from gas as it is strongly affected by electric and magnetic fields while regular gases are not [7]. The use of plasma to improve surface energy and adhesion properties is well established with studies going back as far as in 1969 [8]. In recent years plasma has become a more viable option for surface treatment in the industry with the development of atmospheric pressure, cold plasma. The search for more environmentally friendly methods of surface treatment has also led to a greater use of plasmas due to their high environmental efficiency compared to chemical processes [9]. In [10] the mechanism by which a plasma activates a surface is described. As the plasma bombards the surface, it causes the creation of free radicals through chain scission of molecules. Polar oxygen groups are created on the surface by the radicals reacting with oxygen in the air. Al-Maliki et al. [11] determined that post-treatment there was an increase in oxygen content and a decrease in carbon content forming polar functional groups that increased the wettability of the surface thus making the surface more hydrophilic. They attributed plasma treatment's ability to increase surface energy to the combination of two main factors, increased wettability and increased surface roughness. The plasma treatment may also cause changes in the topography of the surface depending on the type of treatment used and the treatment time experienced. Sanchis et al. [12] suggested that the surface roughness increases as a function of time. Samples of polyurethane film were treated for between 1 and 20 minutes with a low-pressure plasma. The change in surface roughness may be different depending on the type of treatment used. In [11] and [13] it was found that using dielectric-barrier discharge (DBD) treatment for one minute causes a flattening of the surface rather than a roughening. Hergelová et al. [14] again found that short treatment times caused flattening, but with extended treatment time, the roughness would start to increase rapidly. All the above studies had consistent results regardless of how the topography changed. This indicates that topography plays a much lesser role in increasing the surface energy than surface

chemistry effects. This change in surface energy, however, deteriorated rapidly and after 48 hours the surface energy had reverted to almost pre-treatment levels. This deterioration is due to the chemical instability of the surface modification as the topography remains unchanged. Many molecules created during treatment are unstable and, if post-treatment the samples are not stored in a vacuum, they are exposed to moist air. The oxygen and water vapour in the air can react with the unstable molecules causing post-plasma functionalization thereby impairing the surface activation [12, 15–19]. Due to this, it is vital that bonding occurs as soon as possible post-treatment.

The use of UV to improve polymer adhesion is a promising although under-researched field. Like plasma treatment, there are many different methods of generating UV radiation. Most research has been performed using excimer UV lasers or UV lamps: the main difference between these two is that a laser is monochromatic, coherent and directional, focusing on very small spots on the surface of the material samples, while a lamp is generally non-monochromatic, non-coherent and multi-directional, lighting up wide areas of the surface. In [20] polymers including PEEK, PPS, PEI and PES were treated with both plasma and a UV excimer laser to compare the effects of each treatment method. For both plasma and UV treatment a substantial increase was seen in lap shear strength when compared to untreated materials. In general, the plasma-treated samples performed slightly better than the UV. PEI and PES both had good lap shear strengths without treatment and responded well to plasma treatment. However, both were unresponsive to UV treatment, showing nearly the same behaviour as when untreated. This indicates that the improvement of adhesion properties using plasma or UV is caused by different mechanisms. In [20] contact angles post-treatment were found to increase. This contradicts the results detailed in [21] and [22]. In both of these studies, contact angles decrease after surface treatment. This discrepancy may be due to the different types of UV treatment used or the increased treatment time. Shi et al. [22] achieved their highest fracture toughness after exposing substrates for 30 minutes while the UV pulse duration in [20] was only 20 ns. Zeiler et al. [20] used an atomic force microscope to measure the roughness of each surface post-treatment and they attributed to an increased roughness a larger bonding area and better conditions for mechanical interlocking. Similar experiments detailed in [23] and [24] used vacuum UV treatment rather than excimer lasers and found that the treatment caused the surface to flatten and smoothen on a microscale. The above papers suggest that the surface topography is not affecting the increase in bonding strength and indicates that it is the secondary effect on chemical bonds that have the largest impact [25]. Shi et al. [22] described what was occurring on the surface as the aromatic ether bonds changing to OH and O-C=O bonds which allow for better adhesion. An important consideration for the viability of a surface treatment in industry is the treatment stability. In [20] it was found that the lap shear strength of UV treated semi-crystalline samples of polymers remained relatively consistent for up to 30 days. This is an advantage of UV treatment with respect to plasma treatment as, currently, a material treated with plasma has to be bonded almost immediately, meaning that surface treatment and adhesive bonding must occur in two very close facilities.

In the present work, Polyphenylene sulfide (PPS), Polyetherimide (PEI) and Polyetherether-ketone (PEEK) carbon fibre reinforced composites subjected to three different surface treatments have been tested: atmospheric plasma, ultraviolet radiation (UV) lamp and isopropanol wiping as a control. Quasi-static (QS) tests were conducted on single lap joints bonded by an epoxy-based film adhesive specifically designed by Henkel for the bonding of thermoplastic substrates. The lap shear strength was evaluated, and the failure mechanisms of the different joints were examined for the range of surface treatments considered. It was found that the performances of the PEEK and PPS joints were considerably improved by

the plasma and UV treatments resulting in cohesive and delamination failures, while PEI was unaffected by the plasma and UV treatments and performed very well throughout. The main novelties associated with this work are the following: the employment of a novel UV system requiring relatively short sample exposure times (10 seconds); a systematic comparison of the effect of atmospheric plasma and UV treatments on thermoplastic composite specimens for which the current technical literature contains relatively few relevant studies [20, 21].

2 Materials and Methods

2.1 Samples Manufacturing

Single lap joints were manufactured using carbon fibre reinforced PPS, PEEK and PEI composite substrates. The substrates were supplied by Henkel Ireland and were made of seven layers of Tencate Cetex TC1100, TC1200 and TC1000 for the PPS, PEEK and PEI respectively. The specimens were prepared and tested in accordance with ASTM D5868 [26]. The geometry of the test specimen is shown in Fig. 1a. The structural adhesive adopted for bonding the substrates was also supplied by Henkel Ireland and was a high performance film adhesive with the commercial name Hysol EA9696. The substrates were initially cleaned with isopropanol, then dried. The adhesive film was inserted between the substrates then the joint was put in an oven where the thermal cycle was applied (a linear ramp up to 120° C in 30 min and then holding for 90 min at 120° C). The substrates were held together with two clamps as shown in Fig. 1b during the curing and the subsequent cooling-down at room temperature.

2.2 Surface Treatments

Three sets of samples were tested. The first set, simply wiped with isopropanol, was used as a reference. For the second set, the bonding areas were treated with atmospheric plasma. This treatment was performed at University College Dublin (UCD) Surface Engineering Laboratory using the system represented in Fig. 2a. The parameters (power, exposure time and height) were optimized to get the best adhesion performance according to preliminary tests (see Table 1). Each area to be bonded received 10 seconds of treatment. An optimum

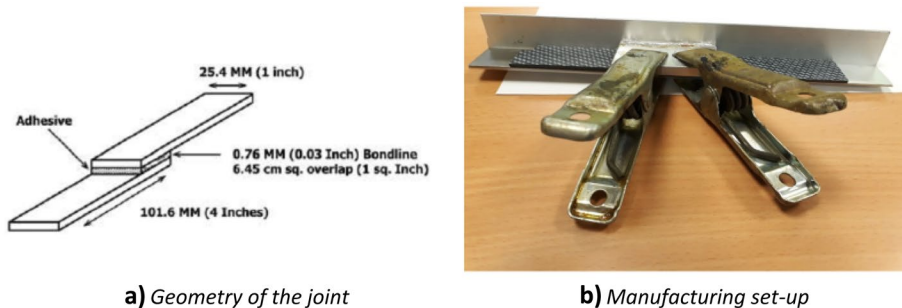
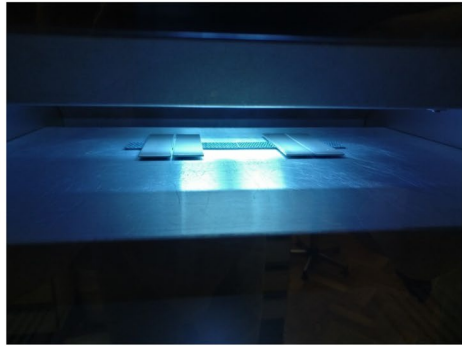


Fig. 1 The specimen geometry and manufacturing set-up



a) *Atmospheric plasma system at UCD*



b) *UV system at Henkel Ireland*

Fig. 2 The surface treatment systems

distance of 12.5 mm between the jet and the material was determined. This procedure was trialled to ensure the substrates were sufficiently treated without causing damage to their surfaces: the absence of damage was verified by optical microscope image analysis of the surfaces of the treated samples. Once treatment was complete, the substrates were wrapped in aluminium foil, and adhesive bonding was performed within 3 hours, bearing in mind the chemical instability of the plasma treatment, as discussed above. For the third set, the bonding areas were UV treated using a system available at Henkel Ireland (Fig. 2b). Samples were placed in a chamber at a fixed distance from the UV Mercury D bulb source (see the parameters in Table 2). The substrates were exposed to UV radiation for 10 seconds and, immediately after, were placed in plastic bags paying extreme attention in not to contaminate them as presented and discussed in [27]. It must be remarked that UV treatment is long lasting (or permanent): previous studies found out that the effect of the surface can remain unaltered for up to three months [28, 29]. After each treatment, the surfaces of the samples were characterized by measuring the free surface energy and the water contact angle. Fourier Transform Infrared spectroscopy (FTIR) and X-ray photoelectron spectroscopy (XPS) were also performed to analyse the surface chemistry of the UV treated samples.

2.3 Lap Shear Strength

The single lap joints were tested using a Hounsfield testing machine. Tabs are square metal sheets 25.4 mm side with the same thickness of the substrates that are applied at the edges

Table 1 Plasma system parameters

Voltage set-up value [%]	95
Plasma voltage [V]	309
Plasma current [A]	14
Plasma power [kHz]	20
Plasma cycle time [%]	100
Height [mm]	12.5
Speed [mm/sec]	100

Table 2 UV lamp treatment parameters

Wavelength	Irradiance
UVV (395–445 nm)	1590 mW/cm ²
UVA (320–390 nm)	1180 mW/cm ²
UVB (280–320 nm)	267 mW/cm ²
UVC (250–260 nm)	36 mW/cm ²

of the specimens for aligning the two tensile forces applied to the joint: the force applied by the moving crosshead and the fixed clamp reaction. Different tests were performed with and without the application of the tabs and changing the overlap length from 25.4 mm (according to [26]) to 6.35 mm (commonly adopted for the tests in Henkel). Every test was performed on five samples.

3 Results and Discussion

3.1 Surface Characterization

The surfaces of the three materials used in the investigation were preliminarily characterized by measuring the contact angles and the free surface energies in each case [30]. These are indicators of the wettability of the material surfaces under examination, even though these parameters in themselves are insufficient to formulate a full and complete evaluation of the adhesion characteristics of the substrates. In Fig. 3 contact angles of the three test liquids used for the characterisation (deionised water, diiodomethane and ethylene glycol) are reported and compared as representative of the surfaces wettability. The free surface energy (see Fig. 4) was evaluated according to the Owens, Wendt, Rabel and Kaelble method (OWRK) [30–32]. From the measurements, the three materials, without any surface treatment, have water contact angles, ranging from around 75 degrees (PEI, PEEK) to around 95 degrees (PPS). This experimental result implies that the untreated surfaces are not wettable and, as a result, they are expected to have relatively poor adhesion properties. Following atmospheric plasma treatment, the water contact angle decreased dramatically to around 20 degrees. This effect was not seen after the UV lamp treatment. In line with the water contact angle measurements, the free surface energies were calculated for the three sets of samples before and after treatment and it was confirmed that the plasma and UV

Fig. 3 Effect of the treatments on the sample surfaces, contact angles

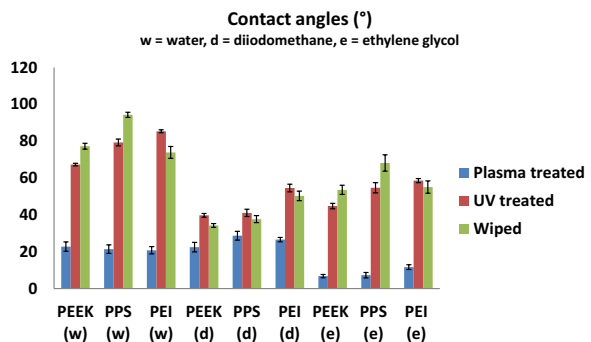
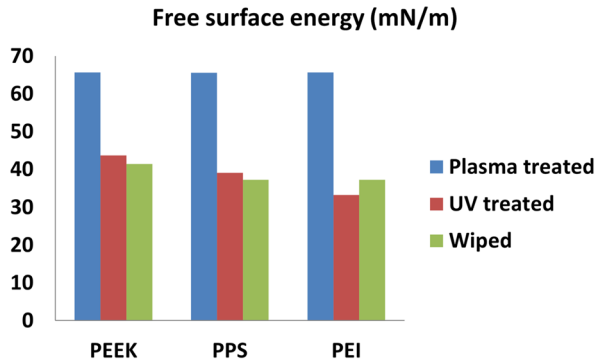


Fig. 4 Effect of the treatments on the sample surfaces, free surface energy



treatments had very different effects on the surface energy values in each case (see Fig. 4). The UV treated surfaces were then analysed by performing FTIR and XPS. The former technique did not reveal significant alterations of the surface properties after the UV treatment while more indications emerged from the XPS analysis. Fig. 5 presents the survey and C1s spectra for PEEK before and after the UV treatment. From these Figures the following conclusions can be drawn: the amount of oxygen atoms increased after UV exposure, while the amount of carbon atoms decreased. From XPS analysis of PEEK samples (see Table 3) the increase of oxygen atomic concentration was from 13.93% to 21.77% while the decrease of carbon atomic concentration was from 83.46% to 73.29%. This would indicate that UV treatment readily forms oxygen-containing groups. This is confirmed by the deconvolution of C1s: after UV exposure, the C-O bonds (286eV) increased; the O-C=O

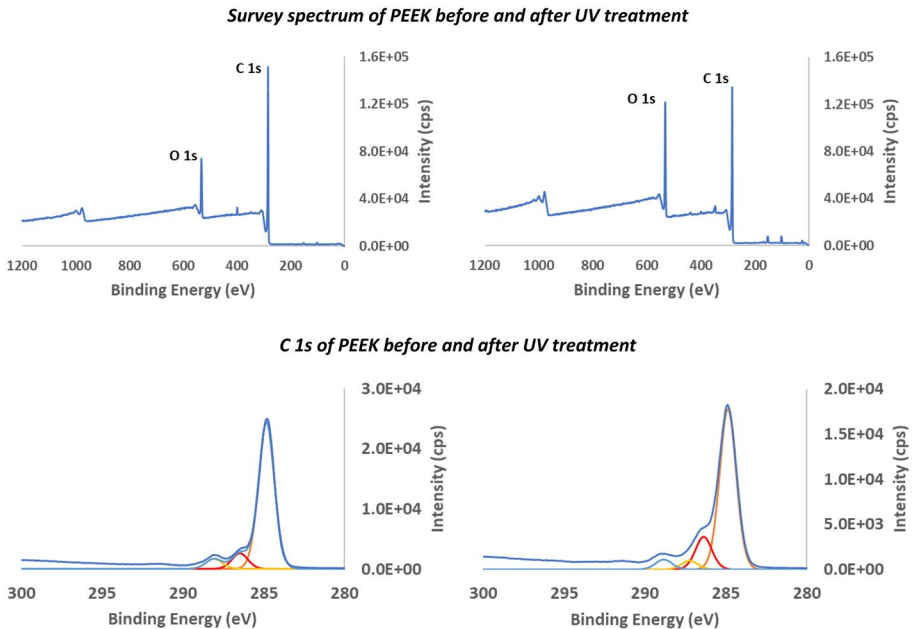


Fig. 5 XPS results on PEEK samples

Table 3 Atomic concentration on the PEEK based samples' (*)

Before UV treatment							
Peak	Position BE (eV)	FWHM (eV)	Raw Area (cps eV)	RSF	Atomic Mass	Atomic Conc %	Mass Conc %
O 1s	533.300	3.870	197429.5	0.780	15.999	13.93	17.51
C 1s	285.300	2.714	447268.5	0.278	12.011	83.46	78.75
After UV treatment							
Peak	Position BE (eV)	FWHM (eV)	Raw Area (cps eV)	RSF	Atomic Mass	Atomic Conc %	Mass Conc %
O 1s	533.300	3.287	329584.6	0.780	15.999	21.77	25.45
C 1s	285.300	2.891	419614.2	0.278	12.011	73.29	64.32

(*) *BE* Binding Energy, *FWHM* Full Width at Half Maximum, *cps* counts per second, *RSF* Relative Sensitivity Factor

bonds (288 eV) increased and a presence of C=O bonds (289 eV) was observed. Similar results were found for PPS.

This alteration of the surface chemistry following the UV treatments can be considered responsible for the improved adhesion properties of the PEEK and PPS composite surfaces. This same result can be found in the technical literature in [28, 29].

3.2 Lap Shear Test Results

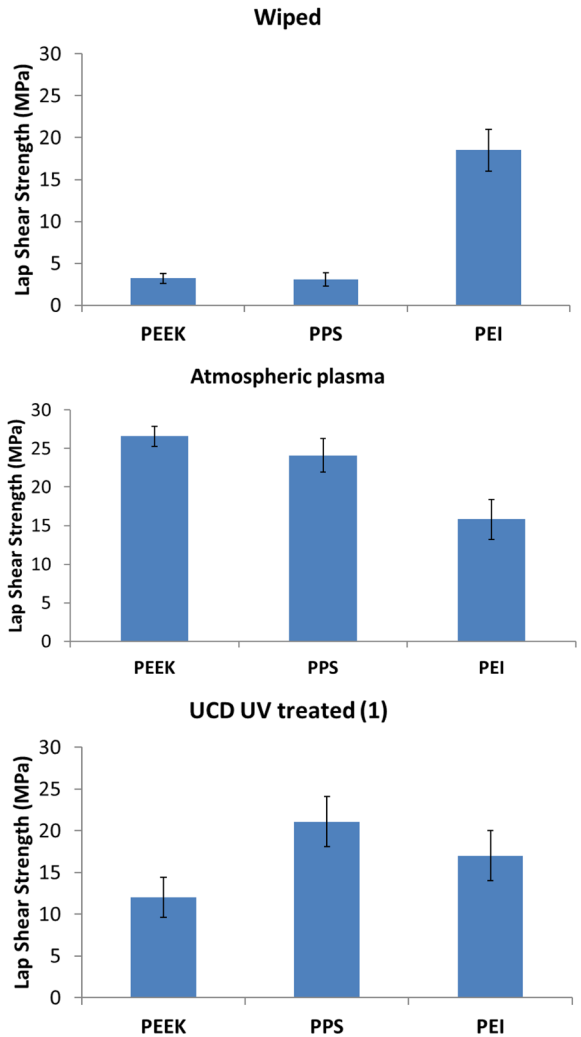
In Fig. 6 the lap shear test results performed on 25.4 mm overlap samples are reported. Simply wiping the bonding areas results in a poor static strength for the two families of samples PEEK, PPS while PEI shows good structural performance even before any kind of surface treatment is applied (see Table 4). Commonly an adhesive joint is defined as structural if its strength is greater than 20 MPa. The fracture surfaces of the different samples were subsequently analysed: the failure was essentially interfacial for PEEK and PPS, indicating poor adhesion between the adhesive and adherend, while the failure for the PEI was mainly cohesive indicating relatively good adhesion between the adhesive and adherend. The lap shear tests were repeated for the samples subjected to the atmospheric plasma treatment.

The results indicated a substantial improvement of the lap shear strength for PPS and PEEK (see the Table 4 for comparison) while PEI samples were essentially insensitive to the treatment or even somewhat negatively affected.

Examination of the fracture surfaces revealed that for the PPS and PEEK samples the failure was mixed delamination/cohesive: in Fig. 7a it is quite clear that the strong adhesion between the adhesive film and the adherend surface, the effect of the atmospheric plasma treatment, resulted in part of the resin being peeled off from the composite sample (delamination) exposing bare fibres.

The examination of the PEI samples revealed a failure mechanism almost identical to that observed before treatment and was essentially cohesive (see Fig. 7b). The tests were then conducted on the UV treated samples. Surprisingly the PEEK specimens revealed a lap shear strength substantially lower than expected - Henkel engineers had previously obtained values of around 34 MPa from an in-house testing programme. The UCD tests indicated that the lap shear strength was 12.0 MPa (average) for the PEEK samples and 21.1 MPa (average) for PPS samples. Some important and meaningful differences arose between the test set-up adopted in Henkel and UCD.

Fig. 6 LSS for the reference and treated samples (25.4 mm)



Firstly, the bonding overlap length for the specimens manufactured at UCD was 25.4 mm while that used for the in-house Henkel tests was 6.35 mm. The second notable difference was the employment of tabs: at the edges of the lap joints tested at UCD, alignment tabs were bonded to minimize the bending moment induced by the misalignment of the tensile forces applied to the specimen’s edges. At the Henkel laboratories, the

Table 4 Results before and after treatment, 25.4 mm overlap (UCD, average LSS in MPa and percent variation)

	Wiping (LSS, reference)	Atmospheric plasma (LSS, percent variation)	UV (LSS, percent variation)
PEEK	3.2 ± 0.6	26.6 ± 1.3 +731%	12.0 ± 2.4 +276%
PPS	3.1 ± 0.8	24.1 ± 2.2 +682%	21.1 ± 3.0 +587%
PEI	18.5 ± 2.5	15.8 ± 2.6 -14%	17.0 ± 3.0 -8%

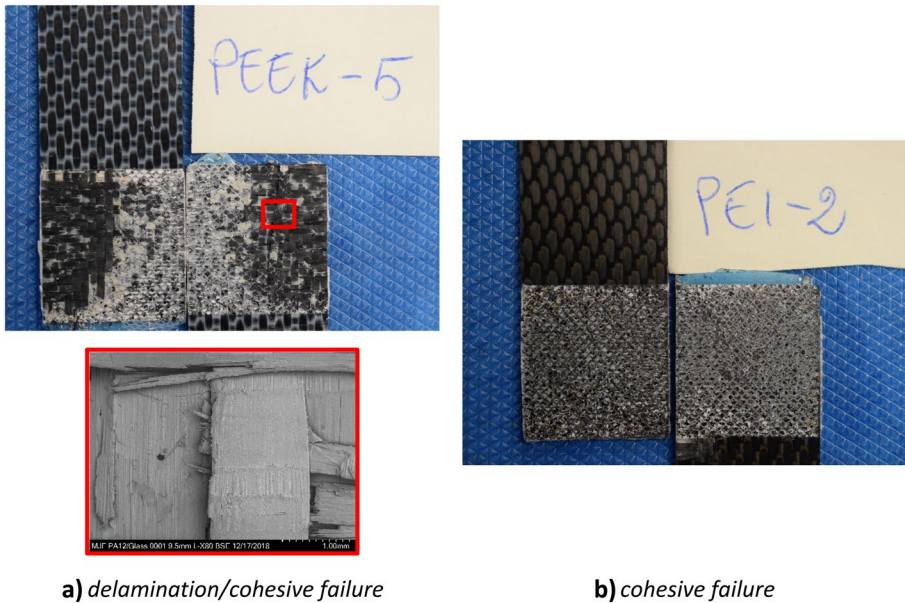


Fig. 7 Fracture surface after plasma treatment

employment of tabs was replaced by the use of self-aligning grips (this configuration is named hereinafter “without tabs (1)”). Another substantial difference was the distance between the two grips of the tensile testing machine clamping the samples (60 mm in Henkel and 125 mm in UCD). This configuration with no tabs and a grip distance of 60 mm is subsequently referred to as “without tabs (2)” (see Fig. 13). Numerical simulations, detailed in the following section, essentially aimed at understanding the effect of the different test setup configurations, were carried out. Hereinafter the experimental results are reported. The lap shear tests were repeated at UCD on samples bonded with an overlap of 6.35 mm. The experimental results found at UCD are reported in the Table 5.

Subsequently the tests were repeated on 25.4 mm overlap samples, removing the tabs from the specimen. This also increased the lap shear strength (18.5 ± 0.3 MPa) although without reaching the values found by the Henkel engineers. Subsequently, the reduction of the distance between the grips, in combination with the removal of the tabs, resulted in a further increase of lap shear strength (22.0 MPa \pm 2.1 MPa), still far from the Henkel values.

SEM images were acquired of the fracture planes for the samples tested at UCD that revealed some important specific features. In Fig. 8 it may be seen that the fracture surface

Table 5 Results after treatment, 6.35 mm overlap (UCD, average LSS in MPa and percent variation respect to 25.4 mm overlap)

	Atmospheric plasma (LSS, percent variation)		UV (LSS, percent variation)	
PEEK	27.7 ± 1.7	+4%	22.5 ± 1.2	+87%
PPS	25.5 ± 1.6	+6%	-	-
PEI	18.8 ± 2.4	+19%	-	-

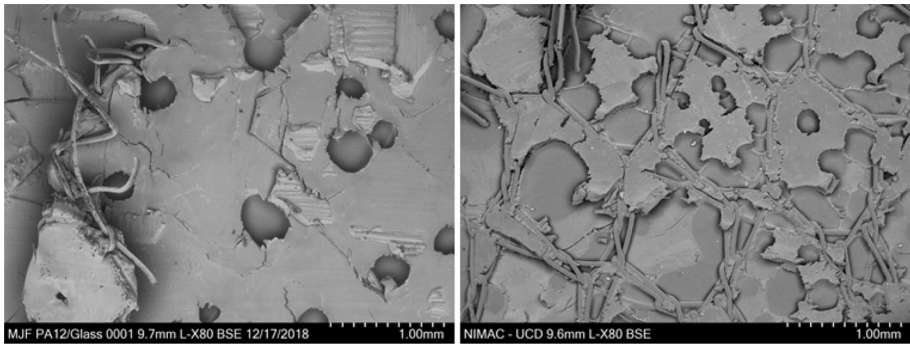


Fig. 8 SEM images of fracture surfaces

was characterized by the presence of holes in the adhesive film layer attached to the composite sample. These holes were mostly confined within a scrim cloth located inside the adhesive film and are indicative of a local poor adhesion. This led to the suspicion that the differences between the UCD and Henkel results may be related to the test specimen fabrication process and the subsequent adhesive curing process itself. The adhesive film was then inspected using SEM microscopy both before and after curing, as shown in Fig. 9. The images of the cured adhesive are presented in which the holes or dimples inside the scrim cloth are clearly evident.

Structural characterization (tensile tests on five dog-bone samples) of the adhesive film layer was performed at UCD to determine the main properties: Elastic modulus, tensile strength, and elongation at break. The samples were prepared by sandwiching one layer of the adhesive between two metallic plates, made non-stick by the application of a polytetrafluoroethylene film. Clamps were applied to the assembly during curing, afterwards removing the epoxy layer and cutting the test samples according to the Standard adopted for the tensile tests [33]. The results are presented in

Table 6a and in Fig. 10a where a typical experimental stress-strain curve is represented.

In an effort to pin-point the cause of the discrepancy between the UCD and the in-house Henkel test results, a visit was made to the Henkel laboratories to observe the in-house process at first hand. There it was observed that the clamps adopted in UCD, while being the same type as those adopted in Henkel, were rather old and well-used and as a result

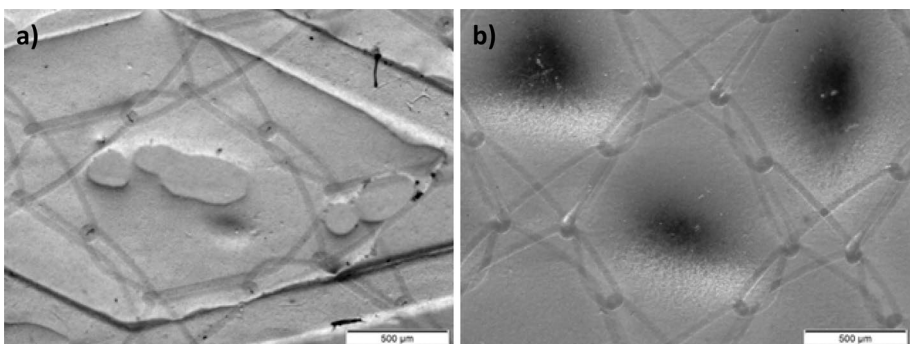


Fig. 9 The adhesive film before (a) and after the curing (b)

Table 6 Adhesive film selected mechanical properties under low and high pressure curing conditions

	a) Adhesive (low pressure)	b) Adhesive (high pressure)
Elastic modulus, E_f (GPa) (*)	0.861 ± 0.124	0.837 ± 0.105
Failure stress (MPa)	15.7 ± 3.1	22.3 ± 1.7
Elongation at break (%)	3.8 ± 1.3	16.0 ± 3.1

(*) Elastic modulus, E_f , of a thin adhesive film is generally different from the bulk Elastic modulus, E .

subjected the test specimens to an applied pressure considerably lower than that applied in Henkel. New tests were conducted at UCD (see Fig. 11) using the Henkel clamps that resulted in the measurement of lap shear strength values broadly in line with what had previously been found in Henkel ($26.5 \text{ MPa} \pm 1.4 \text{ MPa}$). In Fig. 12 the SEM images of the fracture surfaces after UV treatment with appropriate specimen clamping and adhesive curing are reported. Comparison between Fig. 8 and 12 clearly reveals the importance of the clamping process: the stronger pressure applied during the curing process resulted in a more uniform adhesion between the adhesive film and the adherend and the elimination of holes, leading to significantly enhanced structural performance.

Structural characterization of the adhesive film layer was then repeated after an appropriate application of pressure during the adhesive curing process. The results of these tests are reported in Table 6b, where the influence of the clamping pressure on the failure stress and elongation at break is clearly evident: the strength increased on average by 42% and the elongation at break was 4 times greater under the higher pressure curing conditions. The extent of the importance of this parameter on the adhesive strength exceeded our expectations even though an indication of the pressure range to be applied is provided in the product's Technical Data Sheet.

The interpretation of the mechanical behaviour of these three thermoplastic materials before and after treatment can be deduced from the surface analysis in each case and can be also supported in part by the technical literature. The lap shear strength of the PEI samples is actually not governed by the free surface energy, being insensitive

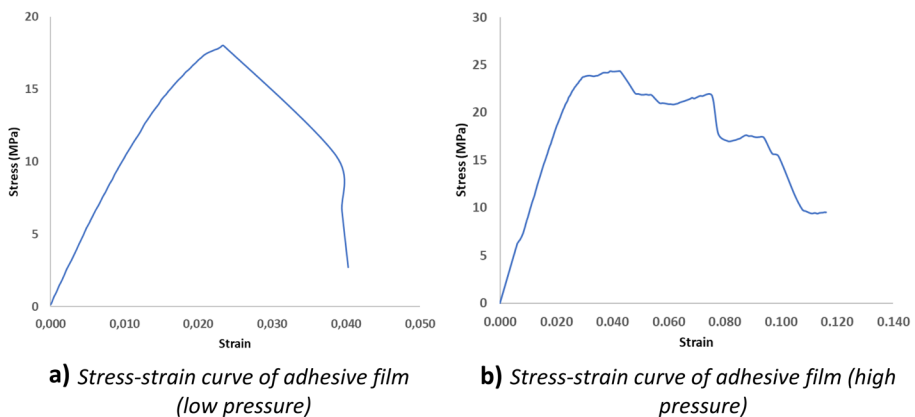
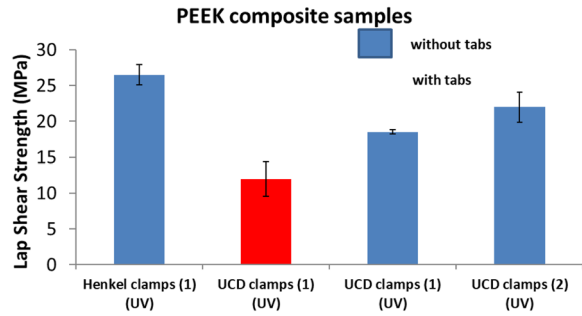
**Fig. 10** Structural adhesive characterization

Fig. 11 LSS results for the different test configurations (25.4 mm overlap)



to both the Plasma and the UV treatments: in all cases investigated, cohesive failure of the adhesive joint was obtained. As reported in [34, 35], curing of an epoxy resin in the presence of PEI can lead to local dissolution of the PEI in the epoxy that results in the formation of a semi-IPN (interpenetrating polymer network) structure at the epoxy-PEI interface. This structure is responsible for a strong interfacial bond that well explains the mechanical results found in the present work. The behaviour of the PPS and PEEK substrates is quite different, however. In the absence of surface treatment, the interfacial failures of the tested samples at low levels of applied load reveal that the epoxy film does not form a strong bond with these materials. As detailed in the introduction section to this paper, the effect of atmospheric plasma treatments is to activate the polymer surface, increasing its free surface energy typically through the addition of polar functional groups. The plasma can also have a role in enhancing surface roughness. This helps to explain the formation of strong bonds between the epoxy adhesive and the thermoplastic samples, leading to the significant increase in the lap shear strength of the joints. The beneficial effects of plasma treatment however tend to be rather short-lived and deteriorate over time. This process is known as hydrophobic recovery and it is associated for example, with the diffusion or reorientation of polar surface groups [36]. In contrast, UV treatments are typically longer term [20], arising from permanent changes to surface chemistry. This can for example be due to the formation of carbonylic groups during the UV treatment, which in-turn can give rise to strong chemical bonding with the epoxy adhesive.

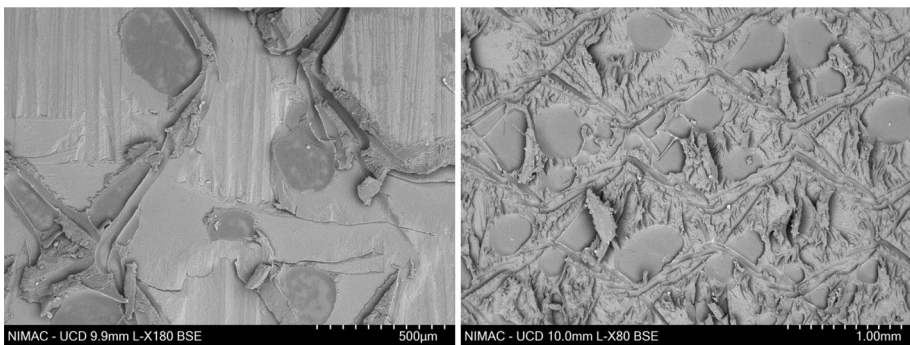


Fig. 12 SEM images of the UV treated PEEK samples fracture surfaces with appropriate application of clamping pressure during the film adhesive curing process

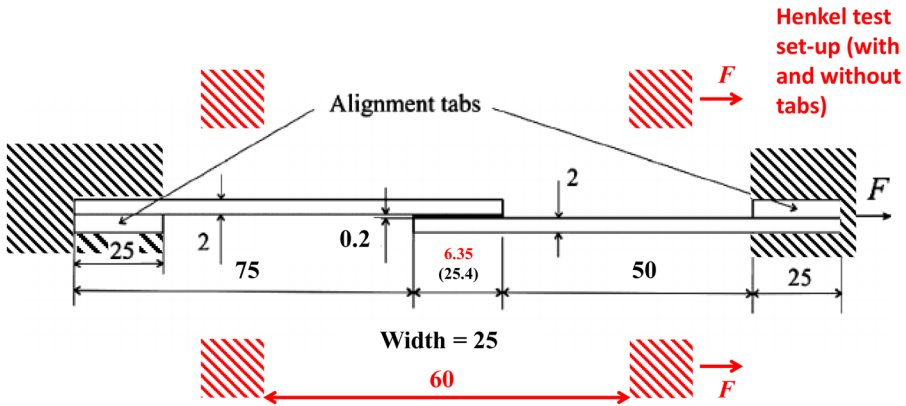


Fig. 13 Geometric configurations adopted for the numerical simulations (dimensions in mm)

3.3 Numerical simulations

Numerical simulations were carried out using Abaqus to analyse the importance of some test set-up parameters on the lap shear strength of the specimens under investigation. For simplicity, isotropic material behaviour was assumed for both the adherends and the adhesive using experimentally determined material properties. Linear elastic, plane stress conditions were also assumed. The typical geometry of the single lap joint is represented in Fig. 13. The overlap length was assumed to be either 25.4 mm or 6.35 mm and the structural analyses were performed with and without alignment tabs. The specimen was constrained at one end imposing clamping conditions representing the application of the grip. At the other end (connected with the load cell and the Hounsfield machine crosshead), a static load was applied, and the nodes were allowed to move freely along the direction 1 of the application of the load. The direction normal to the adhesive layer is denoted direction 2 . With the aim of comparing the stress distributions between the different configurations

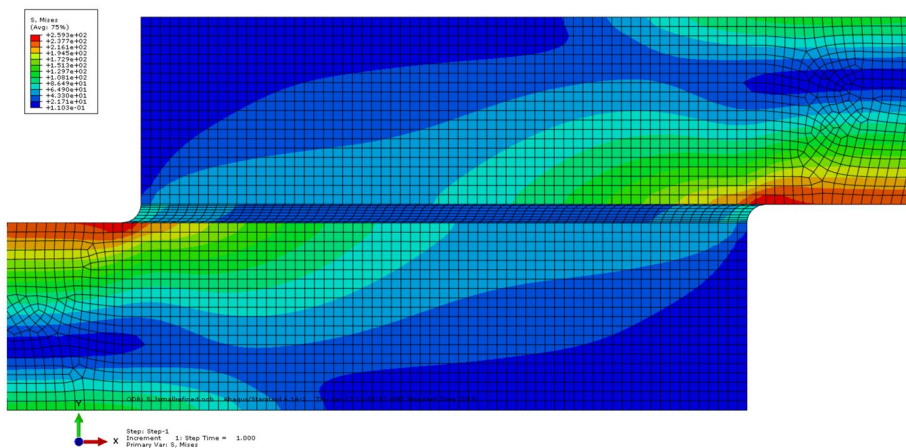


Fig. 14 Typical Von Mises stress distribution in a single lap joint

and the influence of the different parameters on these distributions, the adopted values of the applied static load F were chosen to produce the same average lap shear stress (F/A , where A is the bonded area) for all configurations.

Two different materials were adopted for the simulations: material 1 ($E = 70 \text{ GPa}$, $\nu = 0.33$) for the substrates and the tabs, and material 2 ($E = 3 \text{ GPa}$, $\nu = 0.35$) for the adhesive. The interface nodes between the different materials were simply merged. It must be remarked that this numerical simulation is not intended to reproduce the experimental results but has essentially the scope to:

- 1 evaluate the stress distribution for an overlap of 25.4 mm and 6.35 mm;
- 2 evaluate the influence of the tabs on the test results;
- 3 evaluate the influence of the distance between the grips on the test results.

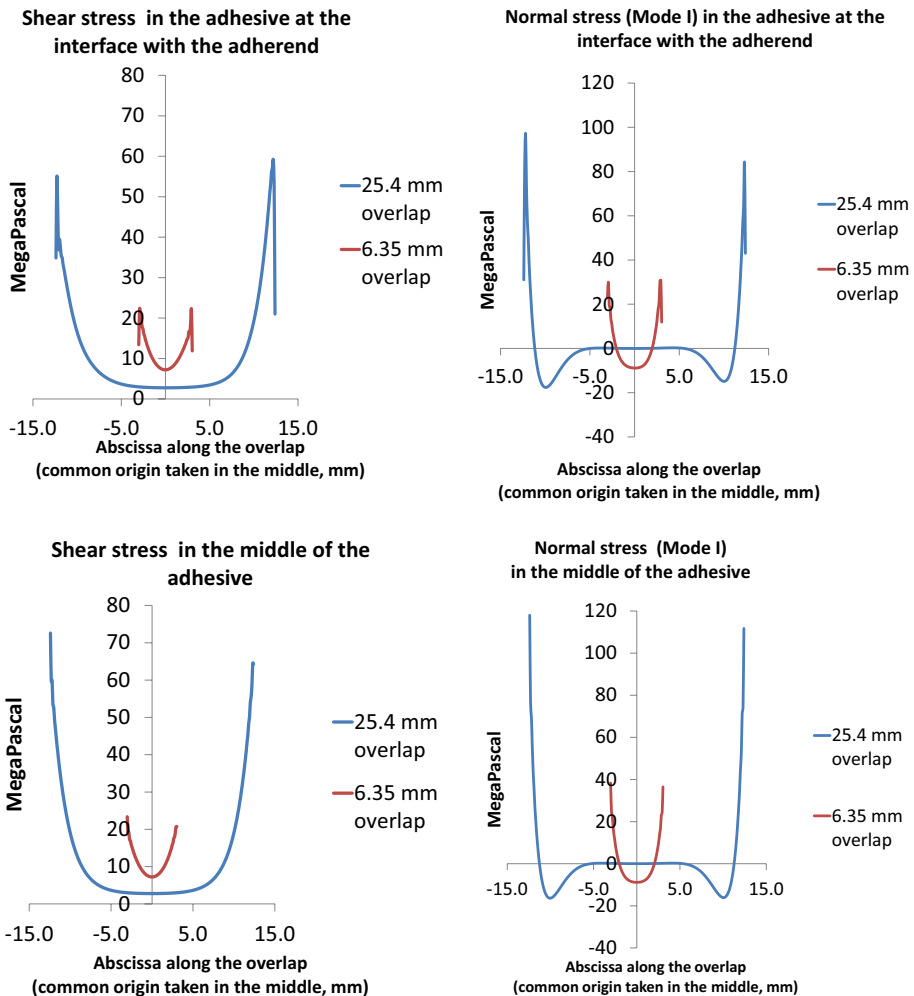


Fig. 15 Normal and shear stress at the locations of interest

Table 7 Overlap length 25.4 mm – stress in the middle of the adhesive (MPa)

	$S_{22,max}$	$S_{12,max}$	$S_{VM,max}$
With tabs	118	73	140
Without tabs (1)	59	37	70
Without tabs (2)	44	29	54

The Von Mises stress has been used as a general indicator of the local stress state together with the normal (Mode I) and shear stress (Mode II). In Fig. 14 the typical stress distribution (Von Mises) around the overlap area is reported. Two locations of interest have been chosen: the interface between the adherend and the adhesive and the middle of the adhesive layer (see Fig. 15). Table 7 and Table 8 report the results for the 25.4 mm and 6.35 mm overlap lengths respectively. The corner between the adherend and the adhesive is a singularity point for the stress, and this is well known from the technical literature [37–41].

The following conclusions can be drawn.

The overlap length has a significant influence on the stress distribution: increasing the overlap length, while keeping the average lap shear stress constant, results in significantly higher peak stresses in the joint. This helps to explain why larger overlaps tend to result in lower experimental lap shear strengths [42]. It is worthwhile to note that lower strength values for larger overlap specimens can also be due to the higher probability of encountering a strength limiting flaw in larger specimens: fibre bundle strengths are generally lower than individual fibres.

The alignment tabs have an outstanding structural effect on the lap shear strength, resulting in an overestimation of the failure load if they are not applied to the specimens: for both overlap lengths, the state of stress is approximately doubled in magnitude when tabs are employed.

Comparing configurations with and without tabs, the normal and shear stress components increase proportionally from one configuration to another. For a given configuration, the normal stress is always dominant respect to the shear stress with a ratio falling in the range 1.5 – 1.6 for each of the different configurations.

If the effective length of the specimen being tested is shortened (i.e., the distance between the two clamps of the tensile machine is reduced), the stress in the adhesive is further mitigated and this effect is more important increasing the overlap length. For an overlap length of 6.35 mm the effective length has almost no effect on the stress distribution.

Table 8 Overlap length 6.35 mm – stress in the middle of the adhesive (MPa)

	$S_{22,max}$	$S_{12,max}$	$S_{VM,max}$
With tabs	38	23	45
Without tabs (1)	19	12	23
Without tabs (2)	18	11	21

4 Conclusions

Single lap joints comprised of carbon fibre reinforced PEEK, PPS and PEI composite substrates and an epoxy film adhesive have been tested to evaluate the effect of a variety of surface treatments on the lap shear strength. The surface chemistry was characterized for the different samples before and after treatment. It was found that both atmospheric plasma and UV treatments considerably increased the lap shear strength of the PEEK and PPS-based composite joints. Atmospheric plasma activated the materials' surfaces, considerably increasing their free surface energies. In contrast, the UV treatment did not significantly change the free surface energy of the samples. XPS conducted on the PEEK and PPS samples after UV treatment revealed the formation of carbonylic groups that may be considered to be responsible for the improved adhesion performance. PEI-based samples were found to be insensitive to the surface treatments or were negatively affected: for this material the lap shear strength is not governed by the free surface energy but by a strong interfacial bond created by its dissolution into the epoxy, forming a semi-interpenetrating polymer network at the epoxy-PEI interface. Limited to this experimental campaign it seems that atmospheric plasma gives slightly better results than UV, but the relatively rapid deterioration of the unstable plasma treated surfaces should be carefully considered when a technical comparison is made. The importance of the pressure applied to the film adhesive during curing was demonstrated and the influence of the test conditions (application of alignment tabs, overlap length and boundary conditions) were assessed using numerical simulation. A follow-up evaluation of the fatigue performance of these joint systems would be of considerable practical importance but was outside the scope of this study.

Open Access This article is licensed under a Creative Commons Attribution 4.0 International License, which permits use, sharing, adaptation, distribution and reproduction in any medium or format, as long as you give appropriate credit to the original author(s) and the source, provide a link to the Creative Commons licence, and indicate if changes were made. The images or other third party material in this article are included in the article's Creative Commons licence, unless indicated otherwise in a credit line to the material. If material is not included in the article's Creative Commons licence and your intended use is not permitted by statutory regulation or exceeds the permitted use, you will need to obtain permission directly from the copyright holder. To view a copy of this licence, visit <http://creativecommons.org/licenses/by/4.0/>.

References

1. Kalpakjian, Serope, Schmid Steven., R.: Manufacturing Engineering and Technology. (2009)
2. Ebnesajjad, S., Ebnesajjad, C.: Surface treatment of materials for adhesive bonding. William Andrew (2013)
3. Rudawska, A.: Surface Treatment in Bonding Technology. Academic Press (2019)
4. Packham, D.E.: Surface energy, surface topography and adhesion. *Int J Adhes Adhes* **23**(6), 437–448 (2003)
5. Kendall, K.: The adhesion and surface energy of elastic solids. *J Phys D App Phys* **4**(8), 1186 (1971)
6. Bonn, D., et al.: Wetting and spreading. *Reviews of modern physics* **81.2**, 739 (2009)
7. Deynse, A.V., Morent, R., De Geyter, N.: Surface modification of polymers using atmospheric pressure cold plasma technology, pp. 506–516. *Research Advances, Practical Applications and Educational Aspects*, Polymer Science (2016)
8. Hall, J., Westerdahl, C.A., Devine, A.T., Bodnar, M.J.: Activated gas plasma surface treatment of polymers for adhesive bonding. *J Appl Polym Sci* **13**(10), 2085–2096 (1969)
9. Zhao, Y., Tang, S., Myung, S.-W., Lu, N., Choi, H.-S.: Effect of washing on surface free energy of polystyrene plate treated by RF atmospheric pressure plasma *Polym. Test.* **25**(3), 327 (2006)

10. Pandiyaraj K., Navaneetha, et al.: Adhesive properties of polypropylene (PP) and polyethylene terephthalate (PET) film surfaces treated by DC glow discharge plasma. *Vacuum* **83**,2, 332-339 (2008)
11. Al-Maliki, H., et al.: Effects of atmospheric plasma treatment on adhesion and tribology of aromatic thermoplastic polymers. *Polym Eng Sci* **58**,S1, E93-E103 (2018)
12. Sanchis, M.R., et al.: Characterization of the surface changes and the aging effects of low-pressure nitrogen plasma treatment in a polyurethane film. *Polym Test* **27**(1), 75–83 (2008)
13. Nastuta, A.V., et al.: Surface modifications of polymer induced by atmospheric DBD plasma in different configurations. *J. Optoelectron. Adv. Mater* **10**(8), 2038–2042 (2008)
14. Hergelová, B., et al.: Plasma surface modification of biocompatible polymers using atmospheric pressure dielectric barrier discharge. *WDS* **12**, (2012)
15. Arpagaus, C., Rossi, A., von Rohr, P.R.: Short-time plasma surface modification of HDPE powder in a plasma downer reactor—process, wettability improvement and ageing effects. *Appl. Surf. Sci.* **252**(5), 1581 (2005)
16. Cepeda-Jimenez, C.M., Torregrosa-Macia, R., Martin-Martinez, J.M.: Surface modifications of EVA copolymers by using RF oxidizing and non-oxidizing plasmas. *Surf Coat Technol* **174**, 94 (2003)
17. Drnovska, H., Lapcik, L., Bursikova, V., Zemek, J., Barros-Timmons, A.M.: Surface properties of polyethylene after low-temperature plasma treatment. *Colloid Polym. Sci.* **281**(11), 1025 (2003)
18. Ortiz-Magán, A.B., Pastor-Blas, M.M., Ferrándiz-Gómez, T.P., Morant-Zacaré, C., Martín-Martínez, J.M.: Surface modifications produced by N₂ and O₂ RF plasma treatment on a synthetic vulcanized styrene–butadiene rubber. *Plasmas Polym.* **6**(1), 81 (2001)
19. Ortiz-Magan, A.B., Pastor-Blas, M.M., Martin-Martinez, J.M.: Surface modifications and adhesion of vulcanized SBR rubber treated with RF plasmas of different gases. *J. Adhes.* **80**(7), 613 (2004)
20. Zeiler, T., et al.: Improvement of adhesive bonding of thermoplastic polymers by different surface treatments. *Macromolecular Symposia*, vol. 126, no. 1. Basel, Hüthig & Wepf Verlag (1998)
21. Kaczmarek, H., et al.: Surface modification of thin polymeric films by air-plasma or UV-irradiation. *Surface Science* **507**, 883-888 (2002)
22. Shi, Huajie, Sinke, Jos, Benedictus, Rinze: Surface modification of PEEK by UV irradiation for direct co-curing with carbon fibre reinforced epoxy prepregs. *Int J Adhes Adhes* **73**, 51–57 (2017)
23. Lapshin, R.V., et al.: Vacuum ultraviolet smoothing of nanometer-scale asperities of Poly (methyl methacrylate) surface. *Journal of Surface Investigation. X-ray, Synchrotron and Neutron Techniques* **4**,1, 1-11 (2010)
24. Pavlenko, V.I., et al.: Effect of vacuum ultraviolet on the surface properties of high-filled polymer composites. *Inorg. Mater. Appl. Res* **5**(3), 219–223 (2014)
25. Wang, Z.K., et al.: Polymer hydrophilicity and hydrophobicity induced by femtosecond laser direct irradiation. *Appl Phys Lett* **95**(11), 111110 (2009)
26. ASTM International: Standard test method for lap shear adhesion for fiber reinforced plastic (FRP) bonding. *ASTM D5868*. (2014)
27. Crane, R.L., Dillingham, G., Oakley, B.: Progress in the Reliability of Bonded Composite Structures. *Applied Composite Materials* **23**(128), 1–13 (2016)
28. Quan, D., et al.: Significantly enhanced structural integrity of adhesively bonded PPS and PEEK composite joints by rapidly UV-irradiating the substrates. *Composites Science and Technology* **108358** (2020)
29. Quan, D., et al.: Rapid surface activation of carbon fibre reinforced PEEK and PPS composites by high-power UV-irradiation for the adhesive joining of dissimilar materials. *Composites Part A: Applied Science and Manufacturing* **105976** (2020)
30. Owens, Daniel, K., Wendt, R.C.: Estimation of the surface free energy of polymers. *Journal of applied polymer science* **13**,8, 1741-1747 (1969)
31. Kaelble, D.H.: Dispersion-Polar Surface Tension Properties of Organic Solids. *J. Adhesion* **2**, 66–81 (1970)
32. Rabel, W.: Einige Aspekte der Benetzungstheorie und ihre Anwendung auf die Untersuchung und Veränderung der Oberflächeneigenschaften von Polymeren. *Farbe und Lack* **77**(10), 997–1005 (1971)
33. Standard ISO, BS EN. 527-2:1996, BS 2782-3: Method 322: 1994, “Plastics - Determination of tensile property-part 2”.
34. Jang, Jyongsik, Shin, Seunghan: Toughness improvement of tetrafunctional epoxy resin by using hydrolysed poly(ether imide). *Polymer* **36**(6), 1199–1207 (1995)
35. Farooq, Ujala, Teuwen, Julie, Dransfeld, Clemens: Toughening of Epoxy Systems with Interpenetrating Polymer Network (IPN): A Review. *Polymers* **12**(9), 1908 (2020)
36. Abourayana, Hisham, M., Dowling, D.P.: Plasma processing for tailoring the surface properties of polymers. *Surface Energy*; In: Tech Rijeka, Croatia 123-152 (2015)

37. Adams, R.D., Peppiatt, N.A.: Stress analysis of adhesive-bonded lap joints. *J Strain Anal Eng Des* **9**(3), 185–196 (1974)
38. Hart-Smith, L.J.: Adhesive Bond Stresses and Strains at discontinuities and Cracks in Bonded Structures. *J Eng Mater Techno* **100**(1), 15–24 (1978)
39. Hart-Smith, L.J.: Adhesively Bonded Joints for Fibrous Composite Structures, L. Tong and C. Soutis, editors, *Recent Advances in Structural Joints and Repairs for Composite Materials*, Springer Science+Business Media Dordrecht p. 173-210 (2003)
40. Hart-Smith, L.J.: Stress Analysis: A Continuum Analysis Approach, A. J. Kinloch, editor, *Developments in Adhesives - 2*, ed, p. 1-44. Applied Science Publishers, London, (1981)
41. Özer, H.: Structural Adhesive Bonded Joints, H. Özer, editor, *Applied Adhesive Bonding in Science and Technology*, IntechOpen (2018)
42. Park, Jae-Hyun., Choi, Jin-Ho., Kweon, Jin-Hwe.: Evaluating the strengths of thick aluminum-to-aluminum joints with different adhesive lengths and thicknesses. *Compos Struct* **92**(9), 2226–2235 (2010)

Publisher's Note Springer Nature remains neutral with regard to jurisdictional claims in published maps and institutional affiliations.